

Electro-optical and structural properties of Al-doped ZnO nanorod arrays prepared by hydrothermal process

Yang-Ming Lu*, Jian-Fu Tang

Department of Electrical Engineering, National University of Tainan, Tainan city, Taiwan, ROC

ABSTRACT — The undoped and Al-doped ZnO nanostructures were grown on ZnO/glass substrates using a low temperature hydrothermal process. The RF-sputtering method was utilized to prepare ZnO film on the glass substrates as a seed layer for subsequently hydrothermal growth of ZnO nanostructures. The properties of ZnO nanorods were characterized by X-ray diffractometer (XRD), scanning electron microscopy (SEM), and room-temperature photoluminescent spectrometer (PL). The X-ray diffraction patterns show that both undoped and Al-doped ZnO nanorod arrays are grown with (002) preferred orientation. Undoped quasi-aligned ZnO nanorods were successfully synthesized by this method. The current-voltage curves of Al-doped ZnO nanorod arrays exhibited a slightly higher current response than the as-grown ones. This result confirms that N-type doping of aluminum can be accomplished effectively by this method.

INDEX TERMS-- ZnO, doped, hydrothermal, nanorod *

I. INTRODUCTION

In recent years, one-dimensional nano-materials such as nanorod, nanobelts, and nanotube have become the focus of intensive research owing to their exceptional applications in fabrication of nanoscale devices [1]. The ZnO semiconductor has attracted much attention in the bottom-up engineering of nanostructures because of its manifold as an excellent nanostructure-former and its unique electronic properties with a wide band-gap of 3.37 eV as well as a large exciton binding energy of 60 meV [2]. ZnO is a promising optoelectronic material with great potential in the applications for optical detector [3], sensor [4], solar cell [5], short-wavelength UV laser, and blue or green optoelectronic devices [6]. Many processes have been used to prepare ZnO including thermal evaporation [7], pulsed laser deposition (PLD), magnetic enhanced sputter [8], metal-organic chemical vapor deposition (MOCVD) [9], and chemical vapor deposition [10]. However, those processes stated above not only require expensive equipment but also are not suitable for batch-type production. In this study, we synthesized pure and Al-doped ZnO nanorods on the transparent substrate using a simple hydrothermal method and effects of the Al-doped concentration on microstructural, electrical and optical properties of Al doped ZnO nanorods were investigated.

The results indicate that the Al doped ZnO resulted in an increase of photocurrent density, This character is suitable used as an optical-electric devices.

II. EXPERIMENTAL METHODS

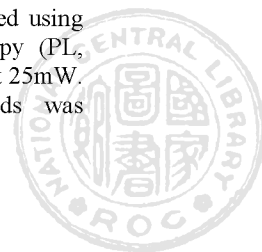
A two-step procedure was used to grow ZnO nanorods from aqueous solution at low temperatures. Firstly, the ZnO thin films were grown by RF sputtering as seed layers for subsequent ZnO nanorods growth. Secondly, the ZnO nanorods were grown from the ZnO seed layer prepared in step one.

For preparation the ZnO seed layers, the substrate temperature was kept at 130 °C. The chamber pressure was 3×10^{-2} torrs with a flow ratio of Ar(95%) and oxygen(5%) mixture gas. The thickness of ZnO seed layers was controlled to be about 100 nm. The solution for growing ZnO nanorods was prepared by mixing of zinc nitrate hexahydrate ($Zn(NO_3)_2 \cdot 6H_2O$) and hexamethylenetetramine (HMT) to give a 0.05M homogeneous solution. The precursor of aluminum dopant trying to be incorporated into ZnO nanorods is aluminum nitrate nonahydrate. Different concentrations of aluminum nitrate nonahydrate ($Al(NO_3)_3 \cdot 9H_2O$) were used to study the influence on the growth and properties of ZnO nanorods. After preparation the solutions, the glass substrates coated ZnO seed layers were immersed in those solutions for growing ZnO nanorods. After keeping 12 hrs at 90 °C for hydrothermal process, ZnO nanorod arrays were successfully grown on the substrate. Finally the samples were taken out from the solution and cleaned with DI water and dried at 60°C.

The structures and morphologies of undoped and Al-doped ZnO nanorods were studied by X-ray diffractometer (Siemens D5000, X-ray Powder Diffractometer) and a field-emission scanning electron microscope (FE-SEM; Hitachi S4800-I). The binding energy level and the chemical bonding of ZnO nanorod arrays were determined by X-ray photoelectron spectroscopy (XPS, Kratos Axis Ulart DLD) with a monochromatic Al K α radiation source at room temperature. The influence of aluminum doping on the optical properties of the ZnO nanorods was studied using room temperature photoluminescence spectroscopy (PL, Shang Wei, FP-6000) with a 325nm He-Cd laser at 25mW. The electrical property of the ZnO nanorods was determined by Hall-effect measurements.

*Corresponding author: ymlu@mail.nutn.edu.tw

DOI : 10.6159/IJSE.2013.(3-2).03



III. RESULTS AND DISCUSSION

3.1 Composition and morphology of ZnO nanorod arrays

To study the effect of Al-dopant concentration on the ZnO nanorods, different precursor concentrations were used. The concentrations of aluminum nitrate nonahydrate ($\text{Al}(\text{NO}_3)_3 \cdot 9\text{H}_2\text{O}$) solutions were chosen as 0.05M, 0.1 M, 0.15M and 0.2M respectively. The aluminum atomic percent in the ZnO nanorods measured by EPMA were 0.4at.%, 0.9at.%, 1.45at.% and 1.67at.% respectively as shown in Fig.1. Comparative morphologies of nondoped and doped ZnO nanorods were shown in Fig.2. Both of them are vertically aligned on the glass substrate with consistently preferred (002) orientation. The Al-doped ZnO nanorods have larger diameter as compared with the undoped ones. Their diameter and length are estimated about 60-80nm and $2 \mu\text{m}$ respectively. ZnO nanorods with larger diameter are expected to be beneficial for optical transmittance as can be seen in Fig.7. Much better transmittance for doped ZnO nanorods compares with the undoped ones. The cross section of the ZnO nanorod demonstrated hexagonal shape implying a well developed crystalline.

3.2 Structure properties of ZnO nanorod arrays

Fig.3 shows the XRD patterns of undoped and Al-doped ZnO nanorods with different dopant concentrations of 0.4at.%, 0.9at.%, 1.45at.% and 1.67at.% respectively. It can be clearly observed, no other compound phase are detected except the peaks from ITO (Indium Tin Oxide) glasses, indicating that the trace Al dopants may have been successfully incorporated into the lattice of ZnO nanorods crystalline. All of them almost orient their c-axis perpendicular to the substrates. The Fig. 4 shows the partially enlarged XRD patterns of these samples with 2θ in the range between 31° and 37° . It can be noted that two faint crystal orientation peaks of (100) and (101) can also be observed for Al-doped ZnO nanorods, and these diffraction peaks can be assigned to the wurtzite hexagonal-shaped ZnO.

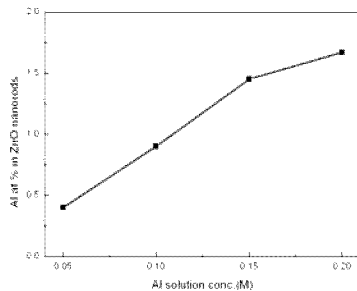


Fig. 1. The aluminum atomic percent in the ZnO nanorods varies with $\text{Al}(\text{NO}_3)_3 \cdot 9\text{H}_2\text{O}$ solution concentration.

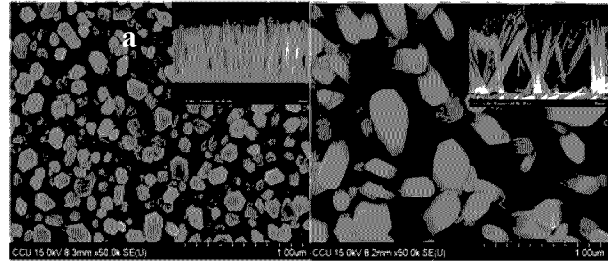


Fig. 2. The SEM images of ZnO doped with nominal concentration: (a) 0at.% and (b) 1.67at.%.

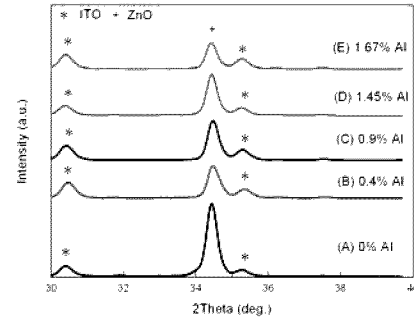


Fig. 3. GIAXRD patterns of the ITO substrate, undoped ZnO nanorod and Al-doped ZnO nanostructures.

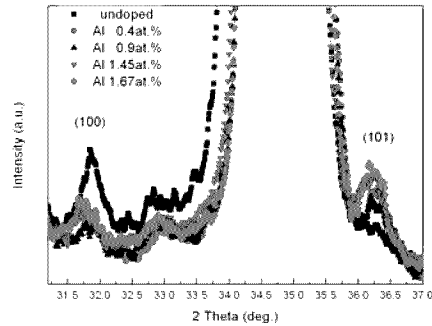


Fig. 4. Shows the partial enlarged XRD patterns of the undoped and Al-doped ZnO nanorods with 2θ in the range between 31° and 37° .

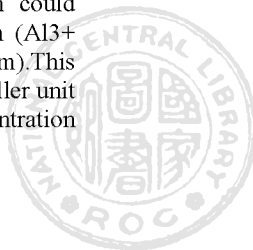
Table 1 summarizes the measured and the calculated data obtained from the XRD curves. The lattice constant and crystal volume of ZnO nanorods, which is calculated according to the relationship:

$$\lambda = 2d_{(hkl)} \sin \theta \quad (1)$$

$$\frac{1}{d^2} = \frac{3}{4} \left(\frac{h^2 + hk + k^2}{a^2} \right) + \frac{l^2}{c^2} \quad (2)$$

$$V_{\text{unitcell}} = \frac{\sqrt{3}}{2} a^2 c \quad (3)$$

where λ is X-ray wavelength, d is spacing between planes of atoms in crystal, θ is Bragg angle, $h k l$ is Miller indices, V is crystal volume. It can be found that the value of the lattice constants "a", the lattice constants "c" and the crystal volume decreases when the Al doping concentration was less than 0.9at.% the Al ion could replace Zn-sites because ionic radius of aluminum ($\text{Al}^{3+} = 0.053\text{nm}$) was smaller than of Zn ($\text{Zn}^{2+} = 0.074\text{nm}$). This displacement will shrink lattices and result in a smaller unit cell. On the contrary, increasing Al doping concentration



beyond 0.9at.%, all the “a”, “c” and crystal volume are increased. This increment could be primarily attributed to excess Al dopants occupy the tetrahedrally and octahedrally interstitial lattice sites when the Al doping concentration is more than 0.9at.% [11]. According to this mechanism, the lattice constant will be enlarged and larger unit cell volume obtained.

Table 1
Lattice constants and crystal volumes of the ZnO nanorods vary with Al doping concentration.

Sample	2θ	Lattice constants		Unit cell volume (nm^3)
		a	c	
0%Al	34.43	0.3247	0.5203	0.04750
0.4%Al	34.45	0.3244	0.5199	0.04738
0.9%Al	34.47	0.3242	0.5197	0.04730
1.45%Al	34.42	0.3248	0.5204	0.04754
1.67%Al	34.40	0.3252	0.5207	0.04769

3.3 Chemical binding of ZnO nanorods

Fig. 5 shows the XPS spectra of ZnO nanorods doping with 0.4at.% and 1.67at.% Al. In Fig. 5(a), it can be found that Zn 2p_{3/2} and Zn 2p_{1/2} are located at 1021.67eV and 1044.9eV, respectively. Fig. 5(b) displays the Al 2p core levels. The binding energy of 74.4 eV is attributed to the Al-O bonds. Although the peak located at 74.4eV is not sharp, it could be speculated that some Al dopants are incorporated into the ZnO nanorods lattices[12].

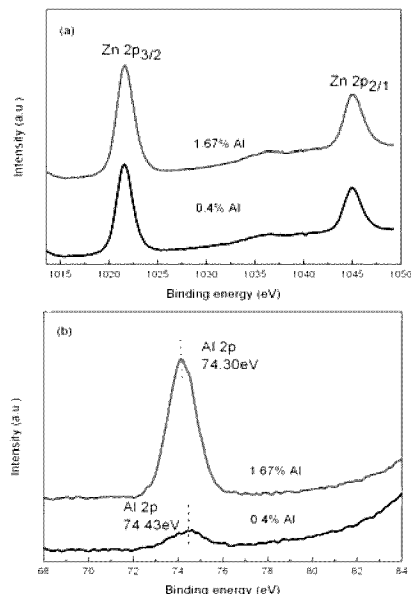


Fig. 5. XPS analysis of ZnO doped with different concentrations of 0.4at.% and 1.67at.% Al:(a) Zn 2p core levels;(b) Al 2p core levels.

3.4 The electrical properties of Al-doped ZnO nanorod arrays

Table 2 shows the carrier concentration, mobilities of undoped ZnO nanorods and Al-doped ZnO nanorods. It was found that, with increasing the Al concentration, the carrier concentration also increased as indicated in table 2. A possible explanation could be stated as follows: When a small amount of Al is introduced into the ZnO nanorods, Al is ionized into Al³⁺ and followed to replace Zn²⁺. Thus one free electron is produced from one Zn²⁺ replacement.

Therefore, the electron concentration increases with the increase in Al concentration [13]. The mobility of ZnO nanorods was found to decrease significantly after Al doping. This might be due to the fact that the Al doping resulted in an increase of ionized impurity scattering centers which obstruct the movement of electrons.

Table 2
Dependence of mobility and carrier density of the ZnO nanorod arrays on the Al-doped concentration.

Sample name	Mobility ($\text{cm}^2/\text{V}\cdot\text{s}$)	Carrier density ($1/\text{cm}^3$)
0%Al	18.96	3.929×10^{14}
0.4%Al	9.8	1.363×10^{16}
0.9%Al	3.75	3.267×10^{17}
1.45%Al	5.16	4.648×10^{17}
1.67%Al	6.34	1.142×10^{18}

3.5 Al-doped ZnO nanorods optical properties

Fig. 6 depicts the room-temperature PL spectra of the undoped and Al-doped ZnO nanorods. Each sample has two types of emission peak; at ultraviolet (UV, ~378nm) and visible (Vis, ~560nm) ranges. The intrinsic emission peak for the ZnO nanorods is observed at 378nm, and that of the Al-doped ZnO nanorods is at 375.5nm. Both peaks are located close to the 2.5nm ZnO band-edge transition. Thus, these two UV emission bands can be ascribed to near band-edge transitions of ZnO nanostructures with wide band gaps, namely, the recombination of free excitons through the exciton-exciton collision process [14]. The transmittance spectra of the Al-doped ZnO nanorod arrays with various Al-doped concentrations are plotted in Fig.7. It was found that, as compared to the undoped ZnO nanorod arrays, the Al-doped ZnO nanorod arrays exhibited significantly improved transmission in the visible region and given a blue shift. According to Burstein-Moss theory [15], the incorporation of Al atoms would provide free carriers to induce the shift of the Fermi level into the conduction band and lead to a larger energy bandgap. The larger energy bandgap would increase the transmission in the visible region [16-17].

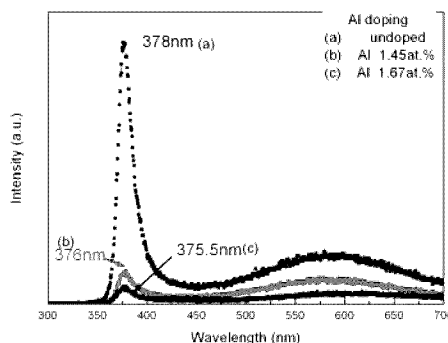


Fig.6. CL spectra of ZnO nanorod arrays with various levels of Al content.



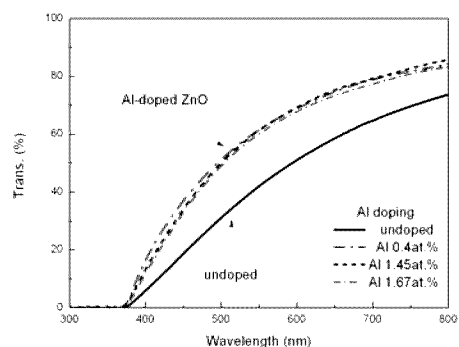


Fig. 7. UV-Vis spectra of ZnO nanorod arrays with various levels of Al concentration.

3.6 Electrochemical Characterization

The photoelectrochemical (PEC) experiments were performed in a rectangular shaped quartz container (80mm x 60mm x 80mm) using a three-electrode system with a platinum gauze (30mm x 20mm) counter electrode, a saturated Ag/AgCl reference electrode and a ZnO nanorods work electrode (15mm x 15mm) immersed in 0.1M KCl and 0.1M LiClO₄ solution. All the data were collected by a ECW-5000 (Jinhan, Taiwan) electrochemical chromatography. The experiments were carried out in the dark and under simulated AM 1.5G solar illumination using a 1000watts Xe-arc lamp. Fig. 8 summarizes the results of the photocurrent density, obtained from ZnO nanorod arrays electrodes in 0.1 KCl and 0.1M LiClO₄ electrolyte with and without the illumination. Obviously, the dark current was lower than the photocurrent, and it was changed very little by applied voltage. It was found that the Al-doped ZnO nanorod arrays exhibited higher current responses than those undoped ones, no matter with or without illumination. The increase in current at a potential of 1.5V of being Al-doped ZnO nanorod arrays with and without illumination could be attributed to the carrier concentration increment after Al doping. Thus, the Al-doped ZnO nanorod arrays are expected to be useful in applications such as electronic devices, photoelectrochemical cells, and electrochemical biosensors.

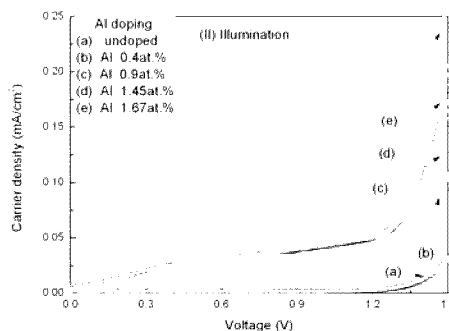
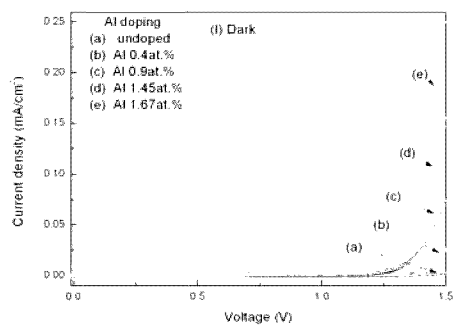


Fig. 8. The current-voltage curves for the ZnO nanorods and the Al-doped ZnO nanorods on dark condition (I)(upper figure) and on illumination condition (II)(low figure).

IV. CONCLUSION

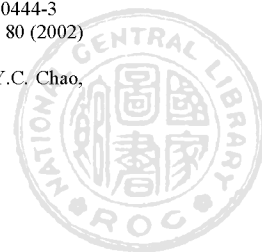
In our work, we successfully grew zinc oxide nanorods on the glass substrate with a ZnO seed layer on it by the hydrothermal synthesis method at much lower temperature. All the ZnO nanorods were vertically aligned on the glass substrates with diameter and length of approximate 60-80nm and 2 μ m, respectively. The aluminum elements were successfully incorporated into ZnO nanorods lattices by using nonahydrate solution as the precursor in the hydrothermal synthesis method. Different amounts of Al (0.4, 0.9, 1.45 and 1.67 at.%) could be doped into the ZnO crystalline lattice. Results indicate that the Al-doped ZnO nanorods have a wurtzite microstructure with c-axis preferred orientation perpendicular to the ZnO seed layer. Al-doped ZnO nanorod arrays with high visible transmittance and carrier density can be obtained. This specific character is suitable used as an electrode material for DSSC, luminescent and electron field emission devices.

ACKNOWLEDGMENT

The authors are grateful to the National Science Council for financially supporting this research under grants NSC100-2221-E-024-007 and 99-2221-E-024-003.

REFERENCES

- [1] Y.N. Xia, P.D. Yang, Y.G. Sun, Y.Y. Wu, B. Mayers, B. Gates, Y.D. Yin, F. Kim, H.Q. Yan, *Adv. Mater.*, 5 (2003) 353-389
- [2] X.D. Gao, X. M. Li, W.D. Yu, L. Li, J.J. Oiu, *Applied Surface Science*, 253 (2007) 4060-4065
- [3] S. Liang, H. Sheng, Y. Liu, Z. Huo, Y. Lu, H. Shen, *Journal of Crystal Growth*, 225 (2001) 110-113. Doi: 10.1023/A:1018527516621
- [4] N. Golego, S.A. Studenikin, M. Cocivera, *Journal of The Electrochemical Society*, 147 (2000) 1592-1594. Doi: 10.1149/1.1393400
- [5] K. Keis, L. Vayssieres, S.E. Lindquist, A. Hagfeldt, *Nanostructured Materials*, 12 (1999) 487-490. Doi: 10.1016/S0965-9773(99)00327-X
- [6] H. Cao, J.Y. Xu, E.W. Seelig, R.P.H. Chang, *Appl. Phys. Lett.* 76 (2000) 2997-2999
- [7] Z.W. Pan, Z.R. Dai, Z.L. Wang, *Science*, 291(2001) 1947-1949. Doi: 10.1016/S0928-4931(01)00293-4
- [8] J.Y. Lee, Y.S. Choi, J.H. Kim, M.O. Park, S. Im, *Thin Solid Films* 403-404 (2002) 553-557. Doi: 10.1016/S0040-6090(02)00444-3
- [9] W.I. Park, D.H. Kim, S.W. Jung, G.C. Yi, *Appl. Phys. Lett.*, 80 (2002) 4232-4234. Doi: 10.1063/1.1499231
- [10] C.L. Wu, L. Chang, H.G. Chen, C.W. Lin, T.F. Chang, Y.C. Chao, J.K. Yan, *Thin Solid Films* 498 (2006) 137-141



- [11] J. Zhang, W. Que, *Solar Energy Materials & Solar Cells*, 94 (2010) 2181–2186
- [12] J.T. Chen, J. Wang, R.F. Zhuo, D. Yan, J.J. Feng, F. Zhang, P.X. Yan, *Applied Surface Science*, 255 (2009) 3959–3964
- [13] M. Eskandari, V. Ahmadi, S.H. Ahmadi, *Physica E*, 42 (2010) 1683–1686. Doi: 10.1016/j.physe.2010.01.024
- [14] S. Yun, J. Lee, J. Yang, S. Lim, *Physica B*, 405 (2010) 413–419
- [15] E. Burstein, *Phys. Rev.* 93 (1954) 632. Doi: 10.1103/PhysRevLett.59.1870.2
- [16] Hur T, Hwang Y, Kim H., *J Appl Phys* 96 (2004) 1507
- [17] Y. Kim, S. Kang, *Materials Letters*, 63 (2009) 1065–1067

BIOGRAPHIES



Professor Yang-Ming Lu (盧陽明) received the master degree from National Taiwan University, Taipei, Taiwan, in 1987 and the Ph.D degree from National Cheng Kung University, Tainan, Taiwan, in 1991. He is an professor since 2002 and transferred to the graduate institute of electro-optical Engineering and served as the director in National Tainan University, Tainan, Taiwan in August, 2007. In 2009, he predominantly merged his institute with the department of electrical engineering and again

served as the chairman of the department till he went to UBC, Canada as a visiting professor for one year in 2011. He also served as a visiting professor at MIT and Harvard University, USA in 2003. He has listed on the Who's Who in the world since 2007. He act as an SCI paper reviewer for lots of famous international journals. He also act as project examine and reexamine committee member of the NSC's projects in the field of electro-optics and materials engineering in Taiwan. He is also the project examiner for the Ministry of Economic Affairs and Science Park in Taiwan.



Jian-Fu Tang (唐健富) got his master degree in department of electrical engineering at University of Tainan in 2011 under the supervision of Prof. Yang-Ming Lu. He continues his research career at National Cheng Kung University being a Ph.D student now.

